ELSEVIER

Journal of Structural Geology 26 (2004) 919–925

JOURNAL OF STRUCTURAL GEOLOGY

www.elsevier.com/locate/jsg

A stress inversion procedure for automatic recognition of polyphase fault/slip data sets

Yehua Shan[a,b,*], Zian Li[b], Ge Lin[b]

[a]Department of Marine Geology, Ocean University of Qingdao, Qingdao City 266003, People's Republic of China
[b]Changsha Institute of Geotectonics, Academic Sinica, Changsha City 410013, People's Republic of China

Received 15 August 2002; received in revised form 20 June 2003; accepted 9 October 2003

Abstract

In deformed rocks fault/slip data are commonly heterogeneous due to variation of the tectonic stress field. Previous methods for separating heterogeneous fault/slip data are based upon hard division, and do not take into account the indeterminable nature of the data. The indeterminability is controlled by many factors such as inaccuracy in the measurement of fault/slip data, heterogeneity of the stress field, and similarity between controlling stress tensors. A new method for separating heterogeneous fault/slip data uses fuzzy C-lines clustering algorithms. It is applied in Fry's (1999) sigma space, in which nonlinear stress inversion is rendered as a solution of hyperlines normal to the girdle of the datum vectors. The method is efficient and quick to make the optimal division and the optimal stress estimates for any chosen division number. From a variety of estimated divisions, the concept of a partition coefficient is introduced (K), which is maximised to determine the best division. As the partition coefficient is only dependent upon the division number and the internal structure of the fault/slip data, the best division obtained in this way is more sound and objective than with previous methods. Two examples illustrate the validity of this method.

Keywords: Polyphase fault/slip data sets; Stress inversion; Fuzzy clustering; Algorithm

1. Introduction

Stress inversion from fault/slip data is an important technique in brittle tectonics for quantification of in-situ palaeostress states in the upper crust (e.g. Carey and Brunier, 1974; Angelier, 1979, 1994; Etchecopar et al., 1981; Armijo et al., 1982; Simón-Gómez, 1986; Huang, 1988; Kleinspehn et al., 1989; Xie and Liu, 1989; Fleischmann and Nemcok, 1991; Hardcastle and Hills, 1991; Will and Powell, 1991; Wojtal and Pershing, 1991; Nemcok and Lisle, 1995; Fry, 1999, 2001; Nemcok et al., 1999; Nieto-Samaniego, 1999; Yamaji, 2000; Lisle et al., 2001; Shan et al., 2003). It assumes homogeneity of the stress field, independence between neighboring faults, and parallelism between the maximum resolved shear on the fault plane and fault striation. Obviously, these assumptions render the conventional inversion technique applicable to homogeneous (or monophase) fault/slip data—a case that the slips recorded on the fault planes occurred in a single phase with the same stress field. However, the tectonic stress field in a region often varies with time by virtue of temporal variation in either far-field forces or near-field forces. Faults in the brittle crust are inherently weak zones, and are readily reactivated in subsequent stress fields (e.g. Nemcok et al., 1999). Therefore, polyphase fault/slip data are more common than monophase fault/slip data in the field. What is more, in the presence of heterogeneous fault/slip data, stress estimated through applying the conventional inversion technique is difficult to interpret (Nemcok and Lisle, 1995).

In order to extend stress inversion techniques to heterogeneous fault/slip data, the critical problem is how to separate the data into homogeneous subsets. Not all methods (e.g. Hardcastle and Hills, 1991; Nemcok and Lisle, 1995; Nemcok et al., 1999; Yamaji, 2000) succeed in this task. We will not elucidate here their potential disadvantages in separating heterogeneous data, but encourage interested readers to refer to the discussion in our paper about a method based on hard division (Shan et al., 2003).

* Corresponding author.
E-mail address: samscoun@public.qd.sd.cn (Y. Shan).

0191-8141/$ - see front matter © 2003 Elsevier Ltd. All rights reserved.
doi:10.1016/j.jsg.2003.10.001

There are two possible shortcomings of existing methods for heterogeneous fault/slip data. First, nearly all these methods specifically pertain to hard division. That is to say, they divide the fault/slip data set into independent subsets, according to some criterion or other. The alternative is called soft division. In reality, the usual nature of fault/slip data, as with many other geological data, is indeterminability. This may be caused by a number of factors such as inaccuracy in the measurement of fault/slip data, heterogeneity of stress field, and similarity between controlling stress tensors. Indeterminability will have an effect on stress estimation, particularly if the controlling stresses are similar to each other (Shan et al., 2003). This is not taken into account by existing methods. Secondly, for a given fault/slip data set, the issue of the optimal number of subsets remains a problem, although it may be determined through analyzing other deformational structures in the region of interest. Apart from the empiricism adopted by most methods, we generally lack a sound objective criterion controlled by internal structure of the fault/slip data set for defining the optimal number of subsets.

The goal of this communication is to try to overcome these shortcomings by presenting a new method based on soft division. In this method, we apply fuzzy clustering to heterogeneous fault/slip data, and define the optimal number of subsets by looking for the maximum partition coefficient under differing subset numbers (no less than two). Two examples demonstrate the validity of the method.

2. New technique

2.1. Fry's (1999) sigma space

In standard inversion methods, the traction caused by stress difference on the fault plane is considered null in direction perpendicular to the striation in inversion methods (Angelier, 1979). The traction equals

$$n\sigma s^{\mathrm{T}} = 0 \tag{1}$$

where σ is the unknown stress tensor, n is the unit vector normal to the fault plane, s is the directional vector perpendicular to the fault striation within the fault plane and the superscript T is the operation of matrix transposition.

Considering symmetry of the stress tensor, Eq. (1) may be rewritten as:

$$\frac{1}{2}\sum_{i=1}^{3}\sum_{j=i}^{3}(2-\delta(i,j))(n_i s_j + n_j s_i)\sigma_{ij} = 0 \tag{2}$$

where $n = [n_1, n_2, n_3]$, $s = [s_1, s_2, s_3]$, σ_{ij} is the element of stress tensor, and $\delta(i,j)$ is the Kronecker delta function. $\delta(i,j)$ equals one when $i = j$ or zero when $i \neq j$.

Let t stand for stress vector $[\sigma_{11}, \sigma_{22}, \sigma_{33}, \sigma_{12}, \sigma_{13}, \sigma_{23}]$ and b for datum vector $[n_1s_1, n_2s_2, n_3s_3, (n_1s_2 + n_2s_1)/2, (n_1s_3 + n_3s_1)/2, (n_3s_2 + n_3s_2)/2]$. Despite its apparently nonlinear feature, Eq. (1) may change into a linear equation after the transformation. In the parameter space—Fry (1999) named it as sigma space—fault/slip data in response to the same tectonic phase will form a hyperplane, or possess a linear structure in sigma space, perpendicular to which is the solution of stress vector. Furthermore, in order to reduce the parameter space without any distortion and to reach a specific solution always requires additional constraints (Fry, 1999; Shan et al., 2003).

For a number of N homogeneous fault/slip data, stress inversion may turn out to be a constrained minimization of an objective function $F(t)$—the sum of the square Euler distances of stress solution to datum vectors. The minimization is:

$$\min F(t) = \sum_{i=1}^{N}(b_i t^{\mathrm{T}})^2 = \sum_{i=1}^{N} t(b_i b_i^{\mathrm{T}})t^{\mathrm{T}} = \sum_{i=1}^{N} tA_i t^{\mathrm{T}}$$
$$= t\left(\sum_{i=1}^{N} A_i\right)t^{\mathrm{T}} = tAt^{\mathrm{T}} \tag{3}$$

subject to

$$tt^{\mathrm{T}} = 1 \tag{4}$$

where b_i is the datum vector related to the ith fault/slip datum, $A_i = b_i b_i^{\mathrm{T}}$, and A is the sum of A_i. The matrices A and A_i are symmetric by definition. Vectors b_i ($i = 1,2,3,\ldots,N$) are normalized to guarantee that each of them has the same contribution to the objective function $F(t)$. For convenience, we will make no difference in notation between the unnormalized and normalized datum vectors. In most cases, the difference between them is relatively minor (see Fry's (1999) tables).

Shan et al. (2003) have proved that in this case, the unit eigen vector having the least eigen value of the matrix is the optimal stress vector.

2.2. Fuzzy classification

In terms of the indeterminability of fault/slip data discussed in the introduction, it is appropriate to consider that they are fuzzy when attributing them to any subsets. The membership of the jth fault/slip vector in the ith subset, or u_{ij}, is a continuous function:

$$u_{ij} \to [0, 1], \qquad i = 1, 2, \ldots, C, \qquad j = 1, 2, \ldots, N \tag{5}$$

$$\sum_{i=1}^{C} u_{ij} = 1, \qquad j = 1, 2, \ldots, N \tag{6}$$

where C is the division number of the fault/slip data set, generally no more than four. Clearly, hard division in which u_{ij} is ether zero or one, is a special case of soft division.

For heterogeneous fault/slip data, the membership of each datum vector is added as weight to the squared Euler distance of the data vector to the stress vector. The objective function is defined as:

$$F(u, t_m) = \sum_{j=1}^{N}\sum_{i=1}^{C} u_{ij}^k D(t_{mi}, b_j)^2 = \sum_{j=1}^{N}\sum_{i=1}^{C} u_{ij}^k \left(b_j t_{mi}^{\mathrm{T}}\right)^2 \qquad (7)$$

where k is the weight exponent (>1), two in the examples below for instance, and $D(t_{mi},b_j)$ is the Euler distance of the jth datum vector b_j to the ith stress estimate t_{mi}. From the above definition we can simply use the fuzzy C-lines clustering algorithm (Bezdek, 1974; Bezdek et al., 1981; Guo and Zhuang, 1993) to minimize the above objective function $F(u,t_m)$. Only the membership and stress estimate are unknown, but none of them can be solved independently. With a stress estimate t_m given, the optimal membership u^* is obtained through optimizing a new composite objective function $P(u,\lambda)$ in which the constraint of Eq. (6) is included:

$$\min P(u, \lambda) = \sum_{j=1}^{N}\sum_{i=1}^{C} u_{ij}^k D(t_{mi}, b_j)^2 - \lambda\left(\sum_{i=1}^{C} u_{ij} - 1\right) \qquad (8)$$

Provided S_{ij}^2 is u_{ij}. Let the partial derivatives of $P(S_{ij},\lambda)$ be zero with respect to S_{ij} and to λ, respectively. Solving these equations, we have an estimate of membership u_{ij}^* with a stress estimate t_m as given:

$$u_{ij}^* = \left[\sum_{l=1}^{C}\left(\frac{D\left(t_{mi}, b_j\right)}{D\left(t_{ml}, b_j\right)}\right)^{\frac{2}{k-1}}\right]^{-1} \qquad (9)$$

With the membership given, the optimal stress estimate t_m^* for each subset is obtained by the method of Shan et al. (2003), as we do with the homogeneous data set in the above section.

In fact, minimization of the objective function is reached by an iterative process such that each of two unknowns is solved independently using the above equation or the above method. The iteration is not terminated until the resolution meets our specification.

The procedure is summarized as follows:

1. Set the division number C (>1), the weight exponent k (>1) and the resolution. The initial stress estimate $t_m^{(0)}$ is given at random. Let $h = 0$.
2. Calculate and normalize the datum vectors from the fault/slip data.
3. Use Eq. (9) to solve the optimal membership $u^{(h)}$, with the stress estimate $t_m^{(h)}$ given.
4. Use the method of Shan et al. (2003) to solve the optimal stress estimate $t_m^{(h+1)}$, with the membership $u^{(h)}$ given, and
5. Compare $t_m^{(h+1)}$ with $t_m^{(h)}$ or $u^{(h-1)}$ with $u^{(h)}$. If the difference between them is outside the required resolution, let $h = h + 1$ and return to step 3. If the difference is at the resolution required, terminate the iteration and output the result.

In the following examples, we set the resolution of the membership of a datum vector in a subset to be 0.001, and the weight exponent to be 2. The above algorithm is very effective and quick to converge (Fig. 1). As our calculation showed, the algorithm seems able to overcome local minima in the parameter space, in that the result at the prescribed resolution bears no relation to the initial value of stress estimate $t_m^{(0)}$.

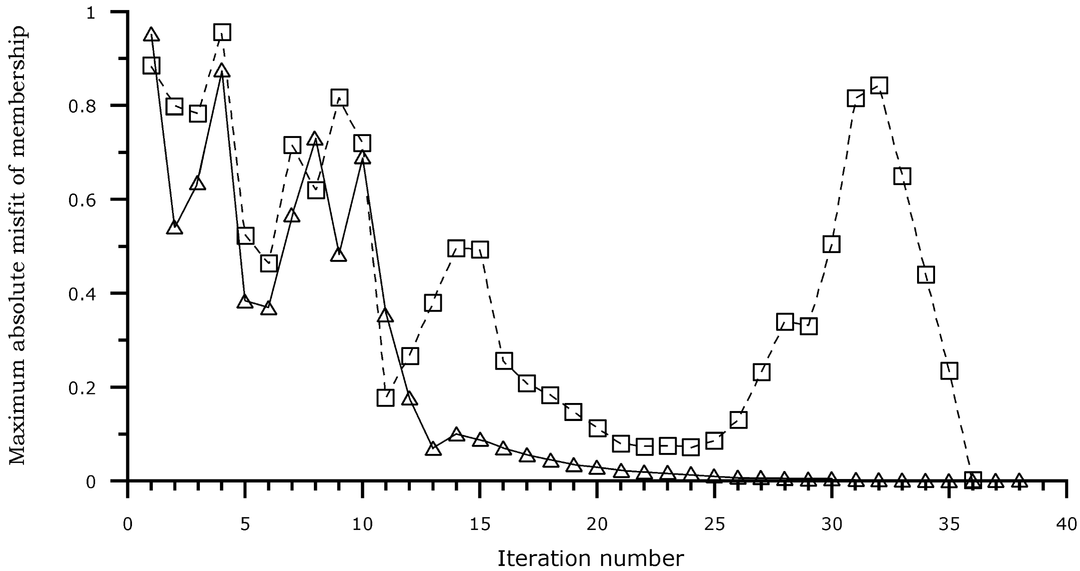

Fig. 1. Maximum absolute misfit of the membership between two neighboring iterations. Short-length dashed line with squares is for case 1 with a division number of three. Line with triangles is for case 2 with a division number of two. See the text for more explanation.

Table 1
Results of the application of our method to case 1. K is the partition coefficient defined in the text. ϕ is defined as $(\sigma_1 - \sigma_2)/(\sigma_2 - \sigma_3)$. See Table 2 for more explanation. W is the percent of fault/slip data in some subsets that have the maximum membership with the subset

		σ_1 (°)		σ_2 (°)		σ_3 (°)		ϕ	K	W
		Bearing	Plunge	Bearing	Plunge	Bearing	Plunge			
Prescribed three subsets	1	180.0	10.0	89.0	5.7	329.9	78.5	2.0		33.33
	2	140.0	5.0	235.0	44.9	45.0	44.7	2.0		33.33
	3	100.0	1.0	195.0	78.7	9.8	11.3	2.0		33.33
Estimated one subset	1	165.5	3.9	257.5	27.3	67.9	62.4	2.0		100.00
Estimated two subsets	1	182.6	10.5	91.0	8.8	321.8	76.3	2.3	0.89	58.33
	2	314.1	10.2	221.9	11.7	84.2	74.3	21.5		41.66
Estimated three subsets	1	180.0	10.0	89.0	5.7	329.9	78.5	2.0	1.00	33.33
	2	140.0	5.0	235.0	44.9	45.0	44.7	2.0		33.33
	3	100.0	1.0	195.0	78.7	9.8	11.3	2.0		33.33
Estimated four subsets	1	303.7	0.0	213.7	0.0	0.0	90.0	13.2	1.00	1.66
	2	180.0	10.0	89.0	5.7	329.9	78.5	2.0		33.33
	3	140.0	5.0	235.0	44.9	45.0	44.7	2.0		31.66
	4	100.0	1.0	195.0	78.7	9.8	11.3	2.0		33.33

2.3. Partition coefficient

The division of heterogeneous fault/slip data, obtained through using the fuzzy C-lines clustering algorithm, varies with the division number chosen. How to determine the best division is a problematic issue for most existing methods for separating heterogeneous fault/slip data. We introduce here the partition coefficient (K) to provide a measure of the acceptability of each division under different division numbers. It is (Bezdek, 1974):

$$K = \sum_{j=1}^{N} \sum_{i=1}^{C} u_{ij}^{*2} / N \tag{10}$$

where K is in a range from $1/C$ to 1. Generally, the larger the value of K, the more acceptable the division. The division with the maximum acceptability is generally considered the best division that we are seeking. This is a comparatively objective criterion that is only dependent upon internal structure of the data.

3. Applications

3.1. Case one

In order to validate the above algorithm, polyphase fault/slip data are simulated for numerically generated monophase sets. Let the validation set of polyphase fault/slip data consist of three monophase subsets, each caused by stress with a stress ratio of two (Table 1). For each tectonic phase, 20 fault/slip data are generated in two steps by Monte-Carlo sampling. In the first step, fault orientations are randomly selected from specific ranges, including fault dip directions ranging from 0 to 360° and dips from 45 to 85°. In the second step, the directions of maximum resolved shear on fault planes are calculated under the given stress tensor within each phase. Therefore, we have a set of 60 artificial fault/slip data with monophase subsets related to three tectonic phases equally mixed (Fig. 2; see appendix 3 of Shan et al. (2003) for the whole data set). The application of our algorithm to them gave the results listed in Table 1.

With a division number of one or two, the partition coefficient is 0.89. The stress estimates are far from the theoretical stresses, and thus meaningless. However, the

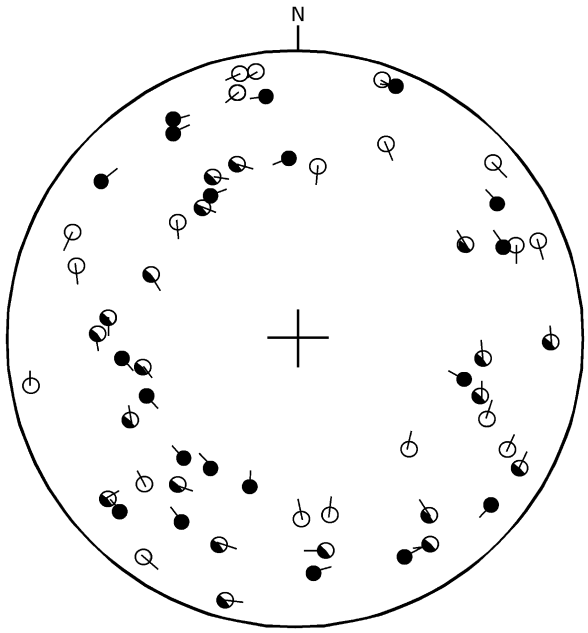

Fig. 2. Lower-hemisphere, equal-area projection of simulated fault/slip data in case 1. Unfilled, half-filled and fully-filled circles represent the normal to fault planes in the category of prescribed subset 1, 2 and 3, respectively. Short lines with an end in the circle center represent the plunges of fault striations.

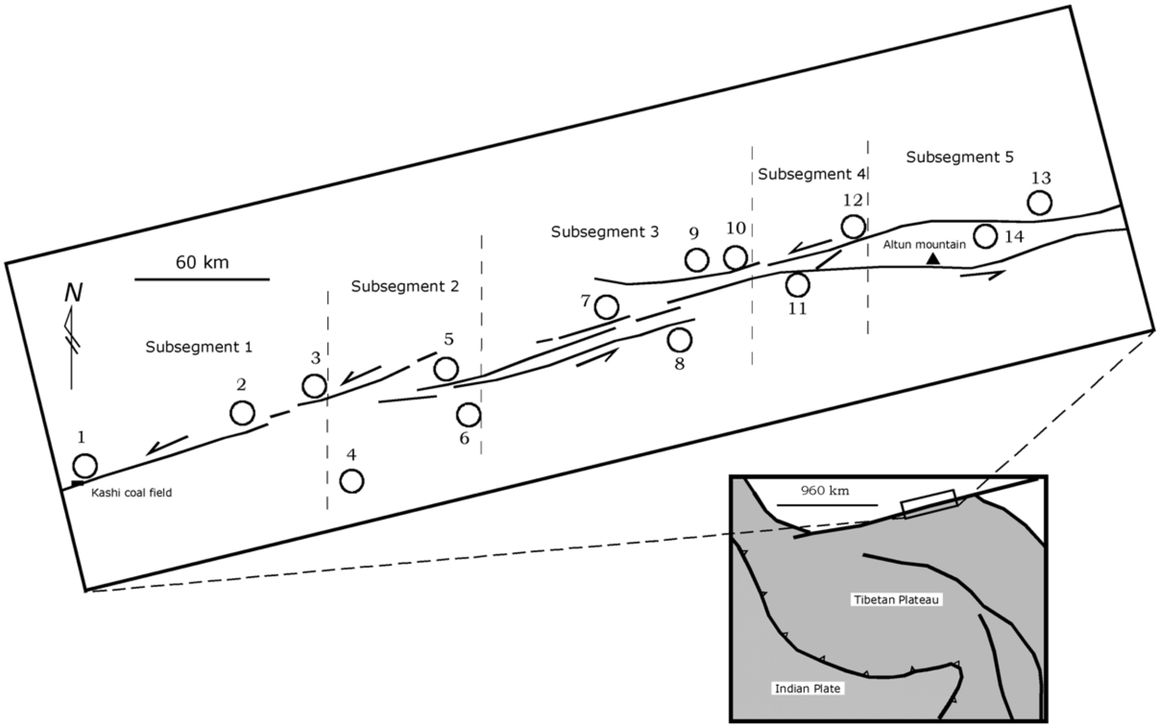

Fig. 3. Subsegmentation of the middle active Altyn Tagh fault, west of China (modified after Xie and Liu (1989)). Labeled circles are the locations for measurement of fault/slip data.

partition coefficient increases with the division number, and reaches one when the division number is three. In this case, stress estimates match theoretical stresses closely. The algorithm has successfully recognized the internal structure of the fault/slip data. Even with a division number of four, we still obtain identical stress estimates, but the new stress estimate has the smallest number of data with maximum membership in the relevant subset. There is no apparent change in partition coefficient. This means that a division number larger than three is not necessary to separate the data set into meaningful subsets. Therefore, without any restraints, we can accept as the best stress estimates those with a division number of three.

3.2. Case two

The active NEE-trending Altyn Tagh fault is one of the most outstanding strike-slip faults in central Asia (Cheng, 1994; Fig. 3). It is about 1600 km in length with a sinistral slip of ca. 350 km, and defines the northern boundary of the

Table 2
Stress estimates in differing locations (Xie and Liu, 1989). Stress ratio R is defined as $(\sigma_1 - \sigma_2)/(\sigma_1 - \sigma_3)$. R and ϕ are related as $1/\phi = 1/R - 1$. Phase 0 took place before the Cenozoic, and only phases 1 and 2 are neotectonic. Phase 1 is earlier than phase 2. See Fig. 3 for each location

Sub-segment	Location	Data number	σ_1 (°)		σ_2 (°)		σ_3 (°)		R	Tectonic phase
			Bearing	Plunge	Bearing	Plunge	Bearing	Plunge		
1	1	9	0.5	37.9	270.2	0.5	179.6	52.1	0.62	1
	2	9	352.9	37.4	188.0	51.7	88.6	7.4	0.64	1
	3	9	10.3	27.6	122.8	36.1	252.8	42.1	0.16	1
2	4	15	54.2	10.4	145.5	7.0	269.1	77.1	0.37	2
	5	6	167.9	10.4	258.4	4.9	3.9	78.9	0.77	1
	6	27	230.2	9.7	140.1	0.7	45.8	80.2	0.28	2
3	7	8	237.4	10.3	329.2	9.6	101.4	75.8	0.00	2
	8	14	50.1	11.1	141.8	8.4	268.1	76.0	0.40	2
	9	6	108.3	13.1	214.4	50.2	8.4	36.8	0.51	0
	10	8	42.8	27.6	144.4	21.1	266.6	54.1	0.08	2
4	11	27	72.2	19.9	284.5	66.9	166.4	11.4	0.09	2
	12	17	219.3	4.8	77.3	83.3	300.7	5.1	0.84	2
5	13	9	54.8	20.2	300.3	39.9	168.2	38.7	0.15	2
	14	34	48.5	16.3	315.8	9.2	197.4	71.4	0.28	2

Table 3
Results of the application of our method to case 2. *W* is the percent of fault/slip data in some subsets that have the maximum membership with the subset

		σ_1 (°)		σ_2 (°)		σ_3 (°)		ϕ	K	W
		Bearing	Plunge	Bearing	Plunge	Bearing	Plunge			
Estimated one subset	1	53.4	9.3	144.4	5.7	265.6	79.1	2.11		100.00
Estimated two subsets	1	166.7	0.7	256.9	16.1	74.5	73.9	1.51	0.82	50.00
	2	72.2	4.2	230.7	85.5	342.0	1.7	110.93		50.00
Estimated three subsets	1	351.1	2.9	260.6	11.2	95.5	78.4	2.46	0.78	29.29
	2	73.4	5.8	175.3	64.0	340.6	25.3	12.27		37.87
	3	59.4	3.4	149.8	7.1	304.0	82.1	0.52		32.82
Estimated four subsets	1	78.7	12.0	199.3	67.4	344.5	12.8	12.78	0.74	30.30
	2	339.0	2.3	248.0	23.1	74.4	66.8	0.59		29.29
	3	227.0	3.6	136.7	6.0	347.9	83.0	1.27		19.69
	4	52.8	28.5	148.1	9.7	255.0	59.6	1.03		20.70

Tibetan Plateau. During the Cenozoic this fault facilitated the extrusion or escape of the thickened Tibetan Plateau created by the continent–continent collision between India and Eurasia (e.g. Molnar and Tapponnier, 1975; Tapponnier et al., 1982; Clark and Royden, 2000).

The middle segment of the Altyn Tagh fault is composed of parallel small-scale strike slip faults that are, to a varying degree, overlapped (Fig. 3). Xie and Liu (1989) divided the middle segment into five subsegments, and in each subsegment measured fault/slip data in fluvial and pluvial sediments of Cenozoic age and to a lesser extent in subjacent older rocks. They applied the 'Etchecopar' software to process the measured data, and obtained two distinct phases, phase 1 and phase 2 (Table 2). The estimated maximum principal stresses in the phases have a small plunge angle, reflecting the compression regime in which fault slip took place. Phase 1 has N–S compression while phase 2 has E–W compression. Phase 1 occurred earlier than phase 2 according to their geological study.

However, the 'Etchecopar' software uses the conventional stress inversion method and does not have the ability to separate heterogeneous data. The work of Xie and Liu (1989) was based upon an implicit assumption that deformation in the form of faulting is spatially heterogeneous and readily forgotten by subsequently overprinting deformation.

The result of our algorithm applied to all of the measured fault/slip data is shown in Table 3. In agreement with Xie and Liu (1989), no matter what the division number is, the estimated principal stresses tend to have a small angle of plunge. With a division number of two, the partition coefficient reaches the maximum. In this case, the bearing of the maximum principal stress is 166.7° in subset 1 and 72.2° in subset 2, representing the approximately N–S and E–W compression. This is consistent with the result of Xie and Liu (1989). Furthermore, our result shows that the estimated minimum principal stress is almost vertical in subset 1 and horizontal in subset 2, and that the stress ratio is far larger in subset 1 than subset 2.

4. Conclusion

Fault/slip data measured in the field are commonly heterogeneous and indeterminable in nature. Particularly for these reasons, the fuzzy C-lines clustering algorithm is employed to separate heterogeneous fault/slip data into many homogeneous subsets. This is feasible because each homogeneous subset tends to have the distribution of a dependent hyperplane in the sigma space. The normal to the hyperplane is the optimal stress vector we solve for. The proposed method allows estimation of both stress and division from heterogeneous fault/slip data, for a given division number. From a number of estimated divisions with varying division number, the concept of a partition coefficient is introduced to determine which division of the data set is the best. The best division is generally considered to be that having the maximum partition coefficient. Two examples were taken to show the feasibility of the method.

Fuzzy clustering algorithms such as the one used in this paper are extremely powerful in detecting internal structures of a data set. We believe they will be of great value in orientation analysis that relies heavily upon visual appreciation (e.g. Ramsay, 1967). Even in stress estimation, more sophisticated algorithms may be used, but this is beyond the scope of the paper.

Acknowledgements

This research was supported by the CAS program (KZCX2-113) and the Shandong NSF (Grant Y98E08078). Most of the work was done in "Laboratory for Numerical Simulation of Continental Deformation and Dynamics" in the Changsha Institute of Geotectonics, Chinese Academy of Sciences. Dr N. Fry at Cardiff University, UK encouraged the first author to translate the paper from Chinese, made a thorough review of the draft and substantially improved the written English of it. This paper was reviewed by J. Miller and R.J. Twiss who made helpful suggestions.

Appendix A

List of symbols and their definitions

Symbol	Definition	Comment
σ	Stress tensor	See Eq. (1)
σ_{ij}	The element of the stress tensor, $i,j = 1,2,3$	See Eqs. (1) and (2)
n	The unit vector normal to the fault plane	See Eq. (1)
n_i	The element of the vector n, $i = 1,2,3$	See Eq. (2)
s	The directional vector perpendicular to the fault striation	See Eq. (1)
s_i	The element of the vector s, $i = 1,2,3$	See Eq. (2)
t	The stress vector	See Eqs. (4) and (5)
b	The vector of fault/slip datum	
b_i	The element of the vector b, $i = 1,2,\ldots,5$	See Eqs. (4) and (7)–(9)
N	The number of fault/slip data	
A_i	The matrix for the ith fault/slip datum, $i = 1,2,\ldots,N$	See Eq. (4)
A	The sum of A_i, $i = 1,2,\ldots,N$	See Eq. (4)
$F(t)$	The objective function for monophase fault/slip data	See Eq. (4)
$F(u,t_m)$	The objective function for polyphase fault/slip data	See Eq. (7)
$P(u,t_m)$	The composite objective function for polyphase fault/slip data	See Eq. (8)
λ	The Lagrange parameter	See Eq. (8)
C	The division number	See Eqs. (5)–(9)
t_{mi}	The ith stress estimate	See Eqs. (7)–(9)
t_m^*	The optimal stress estimates with the membership given	
$t_m^{(h)}$	The optimal stress estimates at the hth iteration	
$D(t_{mi},b_j)$	The Euler distance of the datum vector b_j to the stress estimate t_{mi}, $j = 1,2,\ldots,N$, $i = 1,2,\ldots,c$	See Eqs. (7)–(9)
k	The weight exponent	See Eqs. (7)–(9)
K	Partition coefficient	See Eq. (10)
h	Iteration number	
u_{ij}	The membership of the datum vector b_j in the jth subset	See Eqs. (5)–(8) and (10)
u_{ij}^*	The optimal membership of the datum vector b_j in the jth subset, with the stresses given	See Eq. (9)
$u^{(h)}$	The optimal membership at the hth iteration	
S_{ij}	A square of membership u_{ij}	

References

Angelier, J., 1979. Determination of the mean principal directions of stresses for a given fault population. Tectonophysics 56, T17–T26.

Angelier, J., 1994. Fault slip analysis and palaeostress construction. In: Hancock, P.L., (Ed.), Continental Deformation, Pergamon Press, London, pp. 53–100.

Armijo, R., Carey, E., Cisternas, A., 1982. The inverse problem in microtectonics and separation of tectonic phase. Tectonophysics 82, 145–160.

Bezdek, J.C., 1974. Cluster validity with the fuzzy sets. Journal of Cybernetics 3, 58–73.

Bezdek, J.C., Coray, C., Gunderson, C., Watson, J., 1981. Detection and characterization of cluster substructure. SIAM Journal of Applied Mathematics 40, 339–372.

Carey, M.E., Brunier, M.B., 1974. Analyse theorique et numerique d'un modele mecanique elementaire applique a l'etude d'une population de failes. Compte Rendus Hebdomadaires des Seances de l'Academie des Sciences 279, 891–894.

Cheng, Y.Q. (ed.), 1994. An Outline of Regional Geology in China. Geological Publishing House, Beijing (in Chinese).

Clark, M.K., Royden, L.H., 2000. Topographic ooze: building the eastern margin of Tibet by lower crustal flow. Geology 28, 703–706.

Etchecopar, A., Vasseur, G., Daignieres, M., 1981. An inverse problem in microtectonics for the determination of stress tensors from fault striation analysis. Journal of Structural Geology 3, 51–65.

Fleischmann, K.H., Nemcok, M., 1991. Paleostress inversion of fault/slip data using the shear stress solution of Means (1989). Tectonophysics 196, 195–202.

Fry, N., 1999. Striated faults: visual appreciation of their constraint on possible paleostress tensors. Journal of Structural Geology 21, 7–22.

Fry, N., 2001. Stress space: striated faults, deformation twins, and their constraints on paleostress. Journal of Structural Geology 23, 1–9.

Guo, G.R., Zhuang, Z.W., 1993. Fuzzy Techniques in the Information Processing, Press of National Defense University of Science and Technology, Changsha, (in Chinese).

Hardcastle, K.C., Hills, L.S., 1991. Brute3 and Select: Quickbasic 4 programs for determination of stress tensor configurations and separation of heterogeneous. Computer and Geosciences 17, 23–43.

Huang, Q., 1988. Computer-based method to separate heterogeneous sets of fault-slip data into subsets. Journal of Structural Geology 10, 297–299.

Kleinspehn, K., Pershing, J., Teyssier, C., 1989. Palaeostress stratigraphy: a new technique for analyzing tectonic control on sedimentary-basin subsidence. Geology 17, 253–257.

Lisle, R.J., Orife, T., Arlegui, L., 2001. A stress inversion method requiring only fault slip sense. Journal of Geophysics Research 106, 2281–2289.

Molnar, P., Tapponnier, P., 1975. Cenozoic tectonics of Asia: effects of a continental collision. Science 189, 419–426.

Nemcok, M., Lisle, R.D., 1995. A stress inversion procedure for polyphase fault/slip data sets. Journal of Structural Geology 17, 1445–1453.

Nemcok, M., Kovac, D., Lisle, R.J., 1999. Stress inversion procedure for polyphase calcite twin and fault/slip data sets. Journal of Structural Geology 21, 597–611.

Nieto-Samaniego, A.F., 1999. Stress, strain and fault pattern. Journal of Structural Geology 21, 1065–1070.

Ramsay, J.G., 1967. Folding and Fracturing of Rocks, McGraw-Hill, New York.

Shan, Y., Suen, H., Lin, G., 2003. Separation of polyphase fault/slip data: an objective-function algorithm based on hard division. Journal of Structural Geology 25, 829–840.

Simón-Gómez, J.L., 1986. Analysis of a gradual change in stress regime: example from the eastern Iberian Chain. Tectonophysics 124, 37–53.

Tapponnier, P., Pelfzer, G., Le Dain, A.Y., Armijo, R., Cobbold, P., 1982. Propagating extrusion tectonics in Asia: new insights from simple plasticine experiments. Geology 10, 611–616.

Will, T.M., Powell, R., 1991. A robust approach to the calculation of paleostress fields from fault plane data. Journal of Structural Geology 13, 813–821.

Wojtal, S., Pershing, J., 1991. Paleostress associated faults of large offsets. Journal of Structural Geology 13, 49–62.

Yamaji, A., 2000. The multiple inverse method: a new technique to separate stresses from heterogeneous fault-slip data. Journal of Structural Geology 22, 441–452.

Xie, F.R., Liu, G.X., 1989. Analysis of neotectonic stress field in area of the central segment of Altun fault zone, China. Earthquake Research in China 5, 26–36.(in Chinese with an English abstract).